Mikailalsys Journal of Mathematics and Statistics

e-ISSN : 3030-816X
p-ISSN : 3030-8399

Index : Harvard, Boston, Sydney University, Dimensions, Lens, Scilit, Semantic, Google, etc

https://doi.org/10.58578/MJMS.v4i2.9341

Analysis of the Hydromagnetic Free Convective System in the Presence of Suction/Injection

Umar Muhammad Dauda[1] & Mohammed Umar Mohammed[2]
[1]Kano University of Science & Technology, Kano, Nigeria
[2]Federal University, Dutse, Jigawa, Nigeria
umarmd@kustwudil.edu.ng

Article Info:

Submitted:	Revised:	Accepted:	Published:
Feb 13, 2026	May 11, 2026	May 23, 2026	May 28, 2026

Abstract

This study examines the dynamics of fluid flow and heat transfer under impulsive and accelerated motion conditions in non-steady free convective flow systems. It aims to derive and analyze velocity and temperature profiles under the influence of key physical parameters, including the suction/injection parameter, Grashof number, and Prandtl number. A hybrid analytical–numerical method was employed, integrating Laplace transform-based analytical procedures with numerical evaluation techniques. Two cases of non-steady free convective flow, namely impulsive motion and accelerated motion, were considered. Talbot's method for the inverse Laplace transform was applied in the accelerated motion case to further evaluate the temperature and velocity profiles. The findings show that the suction/injection parameter, Grashof number, and Prandtl number substantially influence both the velocity field and thermal field, thereby shaping the behavior of fluid flow and heat transfer under non-steady convective conditions. This study concludes that the hybrid analytical–numerical approach provides an effective framework for examining transient convective flow problems involving impulsive and accelerated motions. The findings contribute to the literature on fluid

MJMS Journal is licensed under a Creative Commons Attribution-NonCommercial-ShareAlike 4.0 International License

mechanics and heat transfer by offering analytical and computational insights relevant to engineering and thermal science applications.

Keywords: Fluid Flow; Free Convective Flow; Heat Transfer; Laplace Transform; Talbot's Method

Introduction

The study of fluid flow and heat transfer is crucial in many engineering and scientific applications, including energy systems, environmental modelling, and industrial processes. Understanding such fluid behaviour of these systems is essential for optimizing performance and ensuring stability. Hydromagnetic (magnetohydrodynamic) free flows have attracted sustained attention due to wide-ranging applications in those fields mentioned, particularly, cooling of nuclear reactions, mhd power generation, geothermal reservoirs, polymer processing, and microfluidic devices. The interaction between electromagnetic effects and thermal buoyancy forces significantly alters transport phenomena, particularly in boundary-layer flows subjected to external forces such as suction and injection.

Recent studies place emphasis on transient and non-stready flow regimes, where impulsive and accelerated motions better represent real industrial processes compared to steady-state assumptions. Despite the availability of classical boundary layer theories (e.g. Schlichting-type formulations), modern applications demand more refined models incorporating time-dependent behaviour, electromagnetic interactions and coupled thermal fields.

Traditional analytical methods have been effective in solving linear models; however, real-world systems often exhibit nonlinearities that require advanced techniques. A number of studies have analysed MHD free convection flows with suction/injection effects; however, most existing works exhibit at least some limitations such as sole reliance on numerical or analytic approaches which in turn limiting interpretability or generality; or focus on steady or quasiy-steady flows and this usually results in neglecting impulsive and accelerated boundary conditions; and or due to limit exploration of inverse Laplace transform technique that efficiently compute the inversion scheme. Furthermore, existence of few applications of valid analytical-numerical hybrid methods to have sufficient

comparative analysis of sensitive parameters such as Grashof, Prandtl, suction/injection are limited.

This article focuses on analyzing MHD fluid flow problem and heat transfer equations. Although Laplace transform techniques are powerful for such problems, their practical implementation is often constrained by difficulty of inversion. We utilize Laplace transform techniques alongside analytical methods to solve these equations and provide a comprehensive comparison of results. The research considers the effects of key parameters such as the suction/injection parameter, Prandtl number, and Grashof number.

It is apparent that there is need for hybrid approach, numerical-analytical techniques that are capable of handling non-steady MHD free convection flows under the impulsive and accelerated motions; incorporating suction/injection boundary effects; and efficiently computing solutions via numerically stable but robust inverse Laplace technique. In the context of transiet heat transfer, Laplace transform technique remain relevant, as highlighted in several studies, however, faced major challenge lying in the inversion of Laplace-domain solution. Classical approaches are opten computationally unstable or expensive.

Our study addresses these shortcomings by developing and analysing a coupled velocity-temperature system using Laplace transform techniques complemented by Talbot's inversion method, thereby providing both analytical insght and computational robustness. The numerical inversion technique we are implementing was first studied in Abate and Valko (2004) and Weideman (2006). Despite their integration into MHD free convection studies remains limited. Furthermore, suction and injection effects, i.e. the critical in boundary control, have been deeply studied in Gorla and Sidawi (2020), but modern studies rarely combine these effects, the time-dependent impulsive and accelerated boundary conditions.

The dynamics of fluid flow have been widely studied over the years. Classical works by Schlichting (1979) provide a foundation for understanding boundary layer theory. Recent studies have expanded into nonlinear systems, as seen in the work by White (2006), which discusses viscous fluid flow. More recent advances in MHD free convection flows have focused on improving the modelling of coupled thermal-fluid systems under realistic physical considitions.

Studies as reported in articles mostly of International Journal of Heat and Mass transfer and Physics of Fluids and the likes show significant process in the analysis of MHD boundary-layer flows with thermal radiation and viscous dissipation. To mention few, Alkanhal et al. (2019), Abbas et al. (2019) and Ahmed et al. (2019) extensively investigated the MHD nonfluid flows under various physics conditions, demonstrating the importance of magnetic parameters on velocity suppression and heat transfer enhancement. Similarly, T. Hayat et. al. (2019) contributed significantly to nonlinear MHD flows analysis with suction/blowing effects, often employing homotopy analysis perturbation techniques. While these studies provide valuable analytical approximations, they prefequently focus on steady or weakly unsteady flows, limiting applicability to rapidly changing systems.

More recent works by Dharmaiah et. al. (2018); Khan et. al. (2020); Waqas et. al. (2021) have incorporated porous media, chemical reactions, and nanofluids, but often rely heavily on numerical solvers such as finite difference or shooting schemes, with limited validation. Effects of MHD fluid flow parameters are studied in higher dimension and other geometric shapes are studied in Aziz et al. (2021) and Nadeem et al. (2023). Additional studies related to the geometry of the MHD fluid flow at nano levels are found in the following Dogonchi et al. (2019), Ibrahim and Makinde (2015), Tlili et al. (2021).

The Prandtl number and its influence on heat transfer have been explored by Kays and Crawford (1993). Meanwhile, the role of the Grashof number in buoyancy-driven flows is detailed in the studies by Gebhart (1962) and Ostrach (1988). Effect of Grashof number and other related fulid parameter for flow in building environment is studied in Auwal et. al. (2016).

Analytical methods like oscillatory forms and Laplace transform in fluid mechanics have gained attention in recent years, for instance see the work of Jah et. al. (2018) and that of Padmavathi (2023) and Ndolene (2022). The application of these techniques for solving transient heat transfer problems is discussed by ¨Ozisik (1993). Nonlinear models involving suction and injection effects have been examined by Gorla and Sidawi (1994), highlighting the complexity introduced by these parameters.

Studies on the interaction between velocity and temperature profiles are presented in the work of Bejan (2013). Other significant contributions include analytical and

numerical solutions for nonlinear equations by Amanifard et al. (2007) and Shanker et al. (2007).

In a nutshell, the work aims to develop a robust hybrid technique for analysing hydromagnetic free convection flow with suction/injection under impulsive and accelerated motion conditions. This is intended to be achieved via: the formulation of governing equations for transient MHD free convection flow with suction/injection effects; obtain analytical solutions for velocity and temperature profiles via Laplace transform tecniques; implement Talbot's method for efficient numerical inversion; analyse the effects of the key fluid related parameters on the flow behaviour; compare and draw physical implications of the impulsive and accelerated motion cases.

Mathematical Formulation. We are particularly interested in the equations of the form:

$$\frac{\partial \tilde{u}}{\partial \tilde{t}} = \nu \frac{\partial^2 \tilde{u}}{\partial \tilde{y}^2} + v_o \frac{\partial \tilde{u}}{\partial \tilde{y}} + g\beta\left(\tilde{T} - \tilde{T}_\infty\right) - \frac{\sigma B_O^2}{\rho}(\tilde{u} - u_o \gamma \tilde{u}^m) - \frac{1}{\rho}\frac{\partial \tilde{p}}{\partial \tilde{y}} \qquad (1.1)$$

$$\frac{\partial \tilde{T}}{\partial \tilde{t}} = \frac{\kappa}{\rho c_p}\left[\frac{\partial^2 \tilde{T}}{\partial \tilde{y}^2} + \frac{\partial \tilde{p}}{\partial \tilde{y}}\right] + v_o \frac{\partial \tilde{T}}{\partial \tilde{y}} \qquad (1.2)$$

$$\frac{\partial \tilde{p}}{\partial \tilde{y}} = -k_1 \tilde{p} - k_2\left(\tilde{T} - \tilde{T}_\infty\right) \qquad (1.3)$$

where $\tilde{u}, \tilde{T}, \tilde{p}$ are, respectively, the velocity, temperature and pressure profiles of the fluid flow. The system presents an unsteady two dimensional flow problem for an incompressible fluid through an infinite non-conductive porous medium (vertical). The system is assumed to have a uniform magnetic field B_0 being applied in the perpendicular direction ($\tilde{y}$-axis) on the plate while $\tilde{x}$-axis being the vertical direction. We further assume negligible induced magnetic field and therefore, consequent to the very small Reynolds number. We also assume that the initial velocity of the fluid is zero (as it is at rest) with a temperature $\tilde{T}_\infty$.

Along the $\tilde{x}$- direction, the porous plate undergoes an accelerated motion with velocity $u_0\, \tilde{t}^m \gamma$ where $\tilde{t}$ is the associated temporal variable, u_0 is reference velocity/acceleration constant and

$$\gamma = \gamma_o f(t) = \begin{cases} 0, & \text{fixed magnetic } B_o \text{ relative to the fluid} \\ f(t), & \text{fixed magnetic } B_O \text{ relative to the moving porous plate.} \end{cases} \qquad (1.4)$$

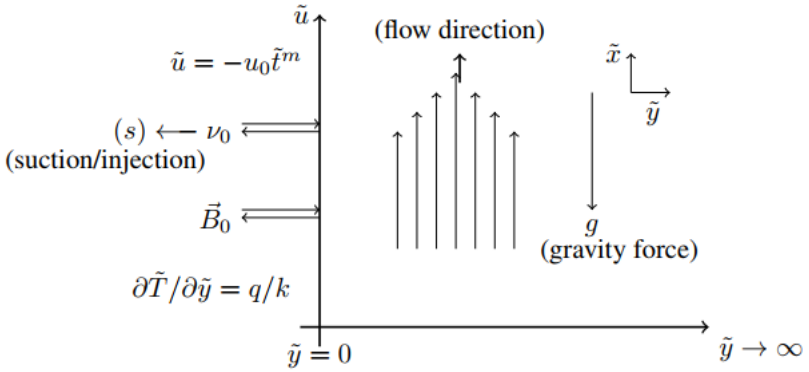


FIGURE 1. The schematic diagram of the convective flow problem.

for an arbitrary well-defined function $f(t)$ for all t. In the scenario where heat is supplied to the plate at constant rate, we take the convective and pressure gradients $\partial\tilde{p}\,/_{\partial\tilde{y}}$ terms in the momentum equation non negligible. The pressure gradient is assumed to be linear in both flow-variables $\tilde{p}$ and $\tilde{T}$ as $-k_1\tilde{p} - k_2\tilde{T}$. The coefficients k_1 represents the pressure growth rate coefficient due to fluid resistance while k_2 is a thermal coupling coefficient effect in a porous media. These coefficients can be defined as in Jah et. al. (2018):

$$k_1 = \frac{q}{k}\left(\frac{\nu^m}{p_0 u_0^{2m-1}}\right)^{\frac{1}{2m+1}}, \qquad k_2 = \left(\frac{u_0^2}{\nu}\right)^{\frac{1}{2m+1}} \tag{1.5}$$

We impose boundary layer approximations on the flow-variable so that the system depends only on the ($\tilde{t}, \tilde{y}$) variables. The explicit solutions of the equation depend on the choice of m with corresponds to impulsive motion when $m = 0$ and accelerated motion when $m = 1$.

Substituting the equation (1.3) into the (1.2) and (1.1), the system narrows down to a set of two equations:

$$\frac{\partial\tilde{u}}{\partial\tilde{t}} = \nu\frac{\partial^2\tilde{u}}{\partial\tilde{y}^2} + \nu_0\frac{\partial\tilde{u}}{\partial\tilde{y}} + g\beta\left(\tilde{T} - \tilde{T}_\infty\right) - \frac{\sigma B_0^2}{\rho}\left(\tilde{u} - u_0\,\tilde{t}^m\gamma\right) + \frac{1}{\rho}\left[k_1\tilde{p} + k_2\left(\tilde{T} - \tilde{T}_\infty\right)\right], \tag{1.6}$$

$$\frac{\partial\tilde{T}}{\partial\tilde{t}} = \frac{\kappa}{\rho c_p}\left[\frac{\partial^2\tilde{T}}{\partial\tilde{y}^2} - k_1\tilde{p} - k_2\left(\tilde{T} - \tilde{T}_\infty\right)\right] + \nu_0\frac{\partial\tilde{T}}{\partial\tilde{y}}. \tag{1.7}$$

Now, the set of equations (1.6) and (1.7) are provided with the following set of conditions

$$\tilde{t} \leq 0: \qquad \tilde{u} = 0, \qquad \tilde{T} = \tilde{T}_{\infty}, \qquad \tilde{y} \geq 0 \tag{1.8}$$

$$\tilde{t} > 0: \begin{cases} \tilde{u} = -u_0 \tilde{t}^m \gamma, & {}^{\partial \tilde{T}}/_{\partial \tilde{y}} = {}^{q}/_{k}, \quad at\ \tilde{y} = 0 \\ {}^{\partial \tilde{u}}/_{\partial \tilde{y}} \to 0, & \tilde{T} = \tilde{T}_{\infty}, \qquad as\ \tilde{y} \to 0. \end{cases} \tag{1.9}$$

To derive the dimensionless form of the equation we introduce dimensionless quantities, u, T, p such that, as similarly found in Jah et. al (2018):

$$\begin{cases} \tilde{t} = (\nu u_0^{-2})^{\frac{1}{2m+1}} t, & \tilde{y} = (\nu^{m+1} u_0^{-1})^{\frac{1}{2m+1}} y, \\ \tilde{T} = \tilde{T}_{\infty} + \dfrac{q\nu}{k u_0} T, & \tilde{u} = (u_0 \nu^m)^{\frac{1}{2m+1}} u. \end{cases} \tag{1.10}$$

Note that, in this case, the characteristic length u0 and characteristic velocity are normalized, thus

$$G_r \sim \frac{g\beta q}{\kappa}.$$

These transformations (1.10) modify the conditions (1.8) to the following:

$$\tilde{t} \leq 0: \quad u = 0, \qquad T = 0, \qquad y \geq 0, \tag{1.11}$$

$$\tilde{t} > 0: \quad \begin{cases} u = -1, & {}^{\partial T}/_{\partial y} = 1, \qquad at\ y = 0 \\ {}^{\partial u}/_{\partial y} \to 0, & T = 0, \qquad as\ y \to \infty \end{cases} \tag{1.12}$$

The nderlying equations are to be analysed subject to these conditions.

Methods

The methodology involves solving the nonlinear equations for velocity and temperature using Laplace transform and analytical methods. The governing equations, derived from conservation laws, are normalized to dimensionless forms for ease of analysis. The impulsive motion case is considered, and boundary conditions are applied to solve the equations. Laplace transform techniques are used to convert the time-dependent partial differential equations into ordinary differential equations. The inverse Laplace transform is

then applied to obtain the time-domain solutions. Analytical solutions are derived for comparison, and MATLAB is employed for numerical implementation and plotting.

Analysis: Impulsive & Accelrated Motions

In both cases of Impulsive and accelerated motions using (1.10), the set of equations are:

$$\left(\frac{u_0^3}{\nu^{1-m}}\right)^{\frac{1}{2m+1}}\frac{\partial T}{\partial t} = \nu\left(\frac{u_o^3}{\nu^{2+m}}\right)^{\frac{1}{2m+1}}\frac{\partial^2 u}{\partial y^2} + \nu_0\left(\frac{u_o^2}{\nu}\right)^{\frac{1}{2m+1}}\frac{\partial u}{\partial y} + \frac{q\nu}{ku_0}\left[g\beta + \frac{k_2}{\rho}\right] - \frac{\sigma B_0^2}{\rho}(u_0\nu^m)^{\frac{1}{2m+1}}(u-\gamma t^m) + \frac{1}{\rho}k_1(p_0\nu^m)^{\frac{1}{2m+1}}p; \quad (4.1)$$

$$\frac{q}{k}\left(\frac{\nu^{2m}}{u_0^{2m-1}}\right)^{\frac{1}{2m+1}}\frac{\partial T}{\partial t} = \frac{k}{\rho c_p}\left[\frac{q}{k}\left(\frac{1}{\nu u_0^{2m-1}}\right)^{\frac{1}{2m+1}}\frac{\partial^2 T}{\partial y^2} - k_1(p_0\nu^m)^{\frac{1}{2m+1}}p - \frac{k_2 q\nu}{ku_0}T\right] + \nu_0\frac{q}{k}\left(\frac{\nu^m}{u_0^{2m}}\right)^{\frac{1}{2m+1}}\frac{\partial T}{\partial y}. \quad (4.2)$$

These equations (4.1)-(4.2) are then reduce to

$$\frac{\partial u}{\partial t} = \frac{\partial^2 u}{\partial y^2} + s\frac{\partial u}{\partial y} + (G_r + \alpha_2)T - \mu(u-\gamma t^m) + \alpha_1 p; \quad (4.3)$$

$$\frac{\partial T}{\partial t} = \frac{1}{P_r}\left[\frac{\partial^2 T}{\partial y^2} - p - T\right] + \frac{\nu_0}{(u_0\nu^m)^{\frac{1}{2m+1}}}\frac{\partial T}{\partial y}. \quad (4.4)$$

where the following fluid related constants are introduced:

$$\begin{cases} s = \frac{\nu_0}{u_0}, \quad \tilde{p} = (p_0\nu^m)^{\frac{1}{2m+1}}, \quad G_r = \frac{g\beta q}{k}.\left(\frac{\nu^{2+m}}{u_0^{2m+4}}\right)^{\frac{1}{2m+1}}, \quad P_r = \frac{\rho c_p}{k}, \\ \mu = \frac{\sigma B_0^2}{\rho}(\nu u_0^{-2})^{\frac{1}{2m+1}}, \quad \alpha_1 = \frac{1}{\rho}k_1\left(\frac{\nu}{u_o^3}\right)^{\frac{1}{2m+1}}, \quad \alpha_2 = \frac{k_2 q}{\rho k}\left(\frac{\nu^{2+m}}{u_0^{2m+4}}\right)^{\frac{1}{2m+1}}. \end{cases} \quad (4.5)$$

In the impulsive case, when $m = 0$, the normalized equation reads

$$\frac{\partial u}{\partial t} = \frac{\partial^2 u}{\partial y^2} + s\frac{\partial u}{\partial y} + (G_r + \alpha_2)T - \mu(u - \gamma) + \alpha_1 p; \qquad (4.6)$$

$$\frac{\partial T}{\partial t} = \frac{1}{P_r}\left[\frac{\partial^2 T}{\partial y^2} - p - T\right] + s\frac{\partial T}{\partial y}. \qquad (4.7)$$

In the accelerated case, where $m = 1$, the equations reads

$$\frac{\partial u}{\partial t} = \frac{\partial^2 u}{\partial y^2} + s\frac{\partial u}{\partial y} + (G_r + \alpha_2)T - \mu(u - \gamma t) + \alpha_1 p; \qquad (4.8)$$

$$\frac{\partial T}{\partial t} = \frac{1}{P_r}\left[\frac{\partial^2 T}{\partial y^2} - p - T\right] + s_0\frac{\partial T}{\partial y}. \qquad (4.9)$$

for a scaled parameter $s_0 = \frac{\nu_0}{(u_0\nu)^{\frac{1}{3}}}$.

Analytic Approach

In this section, we consider analytical solutions of the systems via the use of oscillatory approach and Laplace transform for comparison purpose.

Impulsive case: Oscillatory Form. Here, we consider the set of equations (4.6) and (4.7). Apply the oscillatory form:

$$u = u_0(y)e^{i\omega t}, \qquad T = T_0(y)e^{i\omega t}, \qquad P = \lambda e^{i\omega t}, \qquad \gamma(t) = \gamma_0(y)e^{i\omega t}; \qquad (5.1)$$

Substituting into the momentum and energy equations and simplify, one gets

$$u_0'' + su_0' - (i\omega + \mu)u_0 = -[(G_r + \alpha_2)T_0 + \alpha_1\lambda + \mu\gamma_0]; \qquad (5.2)$$

$$T_0'' + sP_rT_0' - (1 + i\omega P_r)T_0 = \lambda. \qquad (5.3)$$

Solving for $T_0(y)$ yields the solution for u_0 as the equation (5.2) depends on both u_0 and T_0. Since the homogeneous form of the equation (5.3) has solution:

$$T_0^{(h)}(y) = C_-e^{yr_-} + C_+e^{yr_+}, \qquad r_\pm = \frac{-sP_r + \sqrt{s^2P_r^2 + 4(1 + i\omega P_r)}}{2}. \qquad (5.4)$$

Now, taking $\phi_- = e^{yr-}$ and $\phi_+ = e^{yr+}$, we construct the particular solution of the equation (5.3) via the variation of parameter formula:

$$T_0^{(p)}(y) = \phi_+\int \frac{\lambda\phi_-}{W(\phi_-, \phi_+)}dy - \phi_-\int \frac{\lambda\phi_+}{W(\phi_-, \phi_+)}dy$$

where the Wronskian $W\left(\phi_{-,}\phi_{+}\right)$ is defined as:

$$W\left(\phi_{-,}\phi_{+}\right)=\begin{vmatrix}\phi_{-} & \phi_{+}\\ \phi_{-}^{'} & \phi_{+}^{'}\end{vmatrix}=\begin{vmatrix}e^{yr_{-}} & e^{yr_{+}}\\ r_{-}e^{yr_{-}} & r_{+}e^{yr_{+}}\end{vmatrix}=(r_{-}-r_{+})e^{(r_{-}+r_{-})y}\neq 0,\qquad r_{-}\neq r_{+}.$$

Substituting this into the variation of parameter formula, we get

$$T_{0}^{(p)}(y)=\frac{\lambda}{W(r_{+}-r_{-})}\left[e^{yr_{+}}\int e^{-yr_{+}}dy-e^{yr_{-}}\int e^{-yr_{-}}\,dy\right]=\frac{\lambda}{r_{+}r_{-}}$$

$$=-\frac{\lambda}{(1+i\omega P_{r})}. \tag{5.5}$$

where $r_{+}r_{-}=(1+i\omega P_{r})$. Hence, the general solution for (5.3) is

$$T_{0}(y)=T_{0}^{(h)}(y)+T_{0}^{(p)}(y)=C_{-}e^{yr_{-}}+C_{+}e^{yr_{+}}-\frac{\lambda}{(1+iwp_{r})}. \tag{5.6}$$

To fully solve for $T_{0}(y)$ we use boundary conditions for $T_{0}(y)$:

$T_{0}=0,$ at $y\geq 0,\quad T_{0}^{'}(y)=1,$ at $y=0,$ and $\lim_{y\to 0}T_{0}(y)=0.$

By the last and first conditions (respectively), one gets

$$C_{-}+C_{+}=\frac{\lambda}{(1+i\omega P_{r})},$$

$$r_{-}C_{-}+r_{+}C_{+}=0,$$

whose solution yields

$$C_{-}=-\frac{\lambda r_{+}}{(1+i\omega P_{r})(r_{-}-r_{+})},\qquad C_{+}=\frac{\lambda r_{-}}{(1+i\omega P_{r})(r_{-}-r_{+})}.$$

This yields,

$$T_{0}(y)=\frac{\lambda}{(1+i\omega P_{r})}\left[-1-\frac{r_{+}}{(r_{-}-r_{+})}e^{yr_{-}}+\frac{r_{-}}{(r_{-}-r_{+})}e^{yr_{+}}\right] \tag{5.7}$$

Thus, temperature profile $T(t,y)$ is

$$T(t,y)=\frac{\lambda}{(1+i\omega P_{r})}\left[-1-\frac{r_{+}}{(r_{-}-r_{+})}e^{yr_{-}}+\frac{r_{-}}{(r_{-}-r_{+})}e^{yr_{+}}\right]e^{i\omega t}. \tag{5.8}$$

Using the $T_{0}(y)$ in (5.7) above, we solve (4.1) for $u_{0}(y)$ via the variation of parameter with $\phi_{1}(y)=e^{r_{1}y}$ and $\phi_{2}(y)=e^{r_{2}y}$ where

$$r_{1,2} = \frac{-s \pm \sqrt{s^2 + 4(1 - i\omega P_r)}}{2}, \qquad W(\phi_1, \phi_2) = (r_2 - r_1)e^{(r_1 + r_2)y}, \qquad r_1 \neq r_2$$

we get

$$u_0(y) = D_1 e^{r_1 y} + D_2 e^{r_2 y} + e^{r_2 y} \int \frac{e^{r_1 y}(-[(G_r + \alpha_2)T_0 + \alpha_1 \lambda + \mu\gamma_0])}{(r_2 - r_1)e^{(r_1 + r_2)y}} dy$$
$$- e^{r_1 y} \int \frac{e^{r_2 y}(-[(G_r + \alpha_2)T_0 + \alpha_1 \lambda + \mu\gamma_0])}{(r_2 - r_1)e^{(r_1 + r_2)y}} dy$$

This equation is further written as

$$u_0(y) = D_1 e^{r_1 y} + D_2 e^{r_2 y} - \frac{e^{r_2 y}}{(r_2 - r_1)}\left[(G_r + \alpha_2)\int e^{-r_2 y} T_0(y)dy - \frac{(\alpha_1 \lambda + \mu\gamma_0)}{r_2} e^{-r_2 y}\right]$$
$$+ \frac{e^{r_1 y}}{(r_2 - r_1)}\left[(G_r + \alpha_2)\int e^{-r_1 y} T_0(y)dy - \frac{(\alpha_1 \lambda + \mu\gamma_0)}{r_1} e^{-r_1 y}\right] \qquad (5.9)$$

This remains to simplify $\int e^{-r_2 y} T_0(y)dy$ and $\int e^{-r_1 y} T_0(y)dy$ respectively, given that $T_0(y)$ is as defined in equation (5.7).

$$\int e^{-r_1 y} T_0(y)dy = \frac{\lambda e^{-r_1 y}}{(1 + i\omega P_r)}\left[\frac{1}{r_1} - \frac{1}{(r_- - r_+)}\left(\frac{e^{yr_-} r_+}{(r_- - r_1)} - \frac{e^{yr_+} r_-}{(r_+ - r_1)}\right)\right].$$

$$\int e^{-r_2 y} T_0(y)dy = \frac{\lambda e^{-r_2 y}}{(1 + i\omega P_r)}\left[\frac{1}{r_2} - \frac{1}{(r_- - r_+)}\left(\frac{e^{yr_-} r_+}{(r_- - r_2)} - \frac{e^{yr_+} r_-}{(r_+ - r_2)}\right)\right].$$

We therefore write, the solution as

$$u_0(y) = D_1 e^{r_1 y} + D_2 e^{r_2 y}$$
$$+ \frac{\lambda(G_r + \alpha_2)}{(r_2 - r_1)(1 + i\omega P_r)}\left[\frac{1}{r_1} - \frac{1}{(r_- - r_+)}\left(\frac{e^{yr_-} r_+}{(r_- - r_1)} - \frac{e^{yr_+} r_-}{(r_+ - r_1)}\right)\right]$$
$$- \frac{(\square_1 \square + \square\square_0)}{(\square_2 - \square_1)\square_1}$$
$$- \frac{\lambda(G_r + \alpha_2)}{(r_2 - r_1)(1 + i\omega P_r)}\left[\frac{1}{r_2} - \frac{1}{(r_- - r_+)}\left(\frac{e^{yr_-} r_+}{(r_- - r_2)} - \frac{e^{yr_+} r_-}{(r_+ - r_2)}\right)\right]$$
$$+ \frac{(\alpha_1 \lambda + \mu\gamma_0)}{(r_2 - r_1)r_2}.$$

Simplifying further, while taking into account that $r_1 r_2 = -(\mu + i\omega)$ and $(r_2 - r_1)^2 = s^2 + 4(\mu + i\omega)$, we have

$$u_0(y) = D_1 e^{r_1 y} + D_2 e^{r_2 y} + \frac{\lambda(G_r + \alpha_2)}{(r_2 - r_1)(1 + i\omega P_r)}\left[\frac{r_2 - r_1}{r_1 r_2} + \frac{(r_2 - r_1)}{(r_- - r_+)}\left(\frac{r_+ e^{y r_-}}{(r_- - r_1)(r_- - r_2)} - \frac{e^{y r_+} r_-}{(r_+ - r_1)(r_+ - r_2)}\right)\right] + \frac{(\alpha_1 \lambda + \mu\gamma_0)}{(\mu - i\omega)}$$

Now, by using the conditions that

$$u_0(y) = -1 \text{ at } y = 0 \text{ and } \lim_{y\to\infty} u'(y) = 0.$$

By virtue of the first and second conditions, we get

$$D_1 + D_2 = -1 + A_1;$$

$$r_1 D_1 + r_2 D_2 = A_2.$$

where the terms $A_1$and A_2 are defined by

$$A_1 = -\frac{\lambda(G_r + \alpha_2)}{(r_2 - r_1)(1 + i\omega P_r)}\left[\frac{r_2 - r_1}{r_1 r_2} + \frac{(r_2 - r_1)}{(r_- - r_+)}\left(\frac{r_+}{(r_- - r_1)(r_- - r_2)} - \frac{r_-}{(r_+ - r_1)(r_+ - r_2)}\right)\right] + \frac{(\alpha_1 \lambda + \mu\gamma_0)}{(\mu + i\omega)}$$

$$A_2 = -\frac{\lambda(G_r + \alpha_2)}{(r_2 - r_1)(1 + i\omega P_r)}\frac{(r_2 - r_1) r_+ r_-}{(r_- - r_2)}\left(\frac{1}{(r_- - r_1)(r_- - r_2)} - \frac{1}{(r_+ - r_1)(r_+ - r_2)}\right).$$

With these, the values of the coefficients D_1 and D_2 are:

$$D_1 = -\frac{(A_1 + 1)r_2 + A_2}{r_1 - r_2}; \qquad D_2 = \frac{(A_1 - 1)r_1 - A_2}{r_1 - r_2}.$$

Thus, the temperature profile reads:

$$u_0(y) = -\frac{(A_1 + 1)r_2 + A_2}{r_1 - r_2} e^{r_1 y} + \frac{(A_1 - 1)r_1 - A_2}{r_1 - r_2} e^{r_2 y} + \frac{\lambda(G_r + \alpha_2)}{(r_2 - r_1)(1 + i\omega P_r)}\left[\frac{r_2 - r_1}{r_1 r_2} + \frac{(r_2 - r_1)}{(r_- - r_+)}\left(\frac{r_+ e^{y r_-}}{(r_- - r_1)(r_- - r_2)} - \frac{r_- e^{y r_+}}{(r_+ - r_1)(r_+ - r_2)}\right)\right] + \frac{(\alpha_1 \lambda + \mu\gamma_0)}{(\mu - i\omega)}$$

Accelerated Motion Case. Here, we consider the set of equations (4.8) and (4.9). We intend to apply Laplace transform method to solve the equation as follows. Let the Laplace transform of a function $f(t)$ be defined as:

$$\mathcal{L}\{f(t)\} = f(t) = \int_0^\infty f(t)e^{-zt}dt.$$

for a Laplace parameter $z \in \mathbb{C}$.

In this setting, we take the pressure $p(t,y)$ to follow the law $p = p_0 + \alpha T$ for a reference pressure p_0 and $\alpha = \rho R$ with ρ being the fluid density and gas constant R, where $P(z,y) = {}^{p_o}/_{z} + \alpha\hat{T}$ stands for the Laplace transform of $p(t,y)$ and $\hat{T} = \hat{T}(z,y)$ is Laplace trasform of $T(t,y)$.

Upon applying the Laplace transform to both equations and utilizing the linearity property the velocity equation in Laplace domain transform to

$$zU(y,z) - u(y,0) = \frac{d^2U}{dy^2} + s\frac{dU}{dy} + (G_r + \alpha_2)\hat{T}(z,y) - \mu U(z,y) + \frac{\mu\gamma}{z^2} + \alpha_1 P(z,y)$$

Using the initial condition $u(y,0) = 0$:

$$zU(y,z) = \frac{d^2U}{dy^2} + s\frac{dU}{dy} + (G_r + \alpha_2)\hat{T}(z,y) - \mu U(z,y) + \frac{\mu\gamma}{z^2} + \alpha_1 Ps(z,y)$$

This is equivalently written as

$$U'' + sU' - (z+\mu)U = -(G_r + \alpha_2 + \alpha_1\alpha)\hat{T} - \frac{\mu\gamma}{z^2} - \frac{\alpha_1 p_0}{z} \qquad (5.11)$$

The transformed temperature equation is:

$$z\hat{T}(z,y) - T(0,y) = \frac{1}{P_r}\left[\frac{d^2\hat{T}}{dy^2} - P(z,y) - \hat{T}(z,y)\right] + s_0\frac{d\hat{T}(z,y)}{dy}$$

with $\hat{T}(z,y)$ being the Laplace transform of $T(t,y)$. Using the $T(0,y) = 0$, this equation is further simplified t, after suppressing the arguments,

$$\hat{T}'' + s_o P_r\hat{T}' - [(\alpha + 1) + zP_r]\hat{T} = \frac{p_o}{z}.$$

This equation has a solution of the form:

$$\hat{T}(z,y) = E_1 e^{r_3 y} + E_2 e^{r_4 y} - \frac{p_0}{z[\alpha + 1 + zP_r]}, \qquad (5.12)$$

$$\text{where} \quad r_{3,4} = \frac{-s_0 P_r \pm \sqrt{s_o^2 P_r^2 + 4[\alpha + 1 + P_r z]}}{2},$$

for E_1,$E_2$to be determined. Using the boundary conditions in the Laplace domain:

$$U(z,0) = -\frac{1}{z}, \qquad \frac{d\hat{T}}{dy}\Big|_{y=0} = \frac{1}{z},$$

$$\frac{d\hat{T}}{dy}\Big|_{y\to 0} \longrightarrow 0, \qquad \hat{T}(z, y \longrightarrow 0) \longrightarrow 0.$$

One gets:

$$E_1 = \frac{1}{sz} \cdot \frac{sp_o + z(\alpha + 1 + P_r)r_4}{z(\alpha + 1 + zP_r)(r_3 - r_4)}, \qquad E_2 = \frac{1}{sz} \cdot \frac{sp_o + z(\alpha + 1 + P_r)r_3}{z(\alpha + 1 + zP_r)(r_3 - r_4)},$$

and the complete solution reads

$$\hat{T}(z,y) = -\frac{1}{sz} \cdot \frac{sp_o + z(\alpha + 1 + P_r)r_4}{z(\alpha + 1 + zP_r)(r_3 - r_4)} e^{r_3 y} + \frac{1}{sz} \cdot \frac{sp_o + z(\alpha + 1 + P_r)r_3}{z(\alpha + 1 + zP_r)(r_3 - r_4)} e^{r_4 y} - \frac{p_o}{z[\alpha + 1 + zP_r]} \tag{5.13}$$

The inverse Laplace transform of this equation yields:

$$T(t,y) = \int_0^\infty \hat{T}(z,y) e^{zt} dy \tag{5.14}$$

to be computed numerically. With the expression for the $\hat{T}$ obtained, the velocity equation (5.11) has solution, in the Laplace domain,

$$\begin{aligned} U(z,y) = {} & F_1 e^{r_5 y} + F_2 e^{r_6 y} \\ & + e^{r_6 y} \int e^{r_5 y} \frac{G(z,y,s)}{W(e^{r_5 y}, e^{r_6 y})} dy - e^{r_5 y} \int e^{r_6 y} \frac{G(z,y,s)}{W(e^{r_5 y}, e^{r_6 y})} dy = F_1 e^{r_5 y} \\ & + F_2 e^{r_6 y} \\ & - \frac{r_5 e^{(r_5 - r_6)y} - r_6 e^{-(r_5 - r_6)y}}{z^2 r_5 r_6 (r_5 - r_6)(\alpha + 1 + zP_r)} \Big[-(\alpha_1 p_0 z + \mu\gamma_0) r_4 P_r z \\ & + \frac{(G_r + \alpha_1 \alpha + \alpha_2) z}{s(r_3 - r_4)} \big((r_3 r_4 P_r z^2 + (\alpha + 1) r_3 z + s p_0) e^{r_4 y} \\ & - (r_4^2 P_r z^2 + (\alpha + 1) r_4 z + s p_0) e^{r_3 y} - s p_0 (r_3 - r_4) \big) \\ & - (\alpha_1 p_0 z + \mu\gamma_o)(\alpha + 1) \Big], \end{aligned} \tag{5.15}$$

where,

$$r_5 = \frac{-s - \sqrt{s^2 + 4(z+\mu)}}{2}, \qquad r_6 = \frac{-s + \sqrt{s^2 + 4(z+\mu)}}{2},$$

F_1,F_2 are constants to be determined using the boundary conditions while $W(e^{r_5 y}, e^{r_6 y}) = (r_5 - r_6)e^{(r_5+r_6)y}$ and $G(z, y, s)$ is the right-hand-side of the equation (5.11). Then, in the physical space, the $u(t, y)$ is the inverse Laplace transform of $U(z, y)$, where z is the Laplace transform variable:

$$u(t, y) = \int_0^\infty e^{zt} U(z, y) dz.$$

The inverse Laplace transform of $U(z, y)$ and $\hat{T}$(z,y) is computed numerically using MATLAB. We specifically apply *Talbot Contour Method* (TCM) for the evaluation of the integral inverse transform. Talbot's method provides an efficient way to approximate the inverse Laplace transform by contour integration. This document presents an implementation of Talbot's method for solving a physical system modeled by partial differential equations.

Given a Laplace-transformed function $\hat{f}$(s), the inverse Laplace transform is given by:

$$f(t) = \frac{1}{2\pi i} \int_{\sigma - i\infty}^{\sigma + i\infty} e^{zt} \hat{f}(z)\, dz$$

where σ is a finite real number. Talbot's method approximates this integral using a contour transformation:

$$z = \frac{1}{\tan(\theta)} + \frac{1}{\sin(\theta)}, \qquad \theta \epsilon \left[0, \pi/2\right].$$

The numerical integration is performed using the trapezoidal rule and to ensure numerical stability, we impose the following conditions that

- The Prandtl number $P_r \geq 0.2$ to avoid small denominators.
- The suction parameter $s \geq 0.2$ to prevent singular roots.
- The time domain $t > 0.1$ to avoid singularities at $t = 0$.
- The Talbot contour avoids $\theta = 0$ and $\theta = \pi/2$ to prevent division by zero.
- If solutions for F_1 and F_2 are undefined, the system parameters need adjustment.

Results

The velocity and temperature profiles were computed for various values of the suction/injection parameter $\boldsymbol{s}$, Prandtl number $\boldsymbol{P_r}$, and Grashof number $\boldsymbol{G_r}$.

Impulsive case. In this case, the results show that:

• An increase in s leads to a a more stable velocity boundary layer and higher temperature gradients near the surface.

• Higher P_r results in a reduced thermal boundary layer thickness, indicating better heat transfer rates.

• An increase in G_r enhances buoyancy-driven flow, leading to steeper velocity profiles.

Figures 2 and 3 illustrate the effects of these parameters on the profiles.

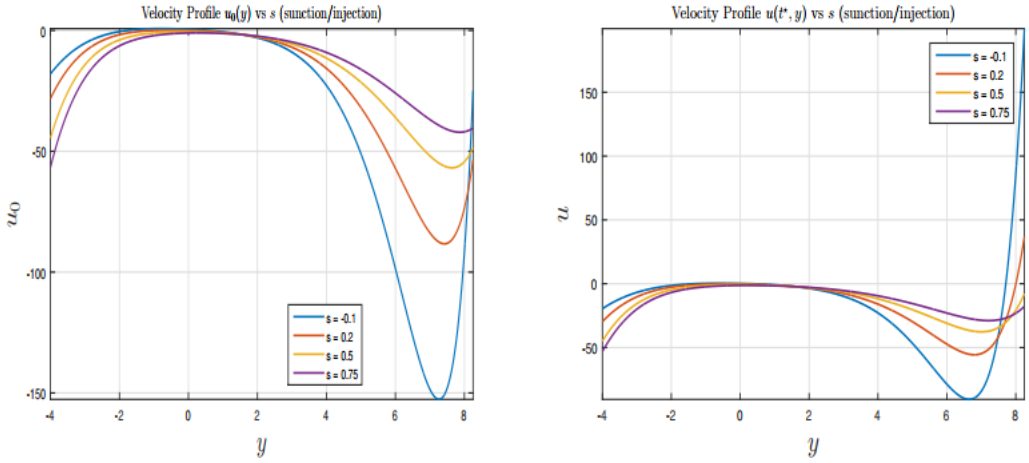


FIGURE 2. velocity profiles for different values of s at $t = 0$ and $t = 0.25$ respectively for fixed values of G_r, P_r.

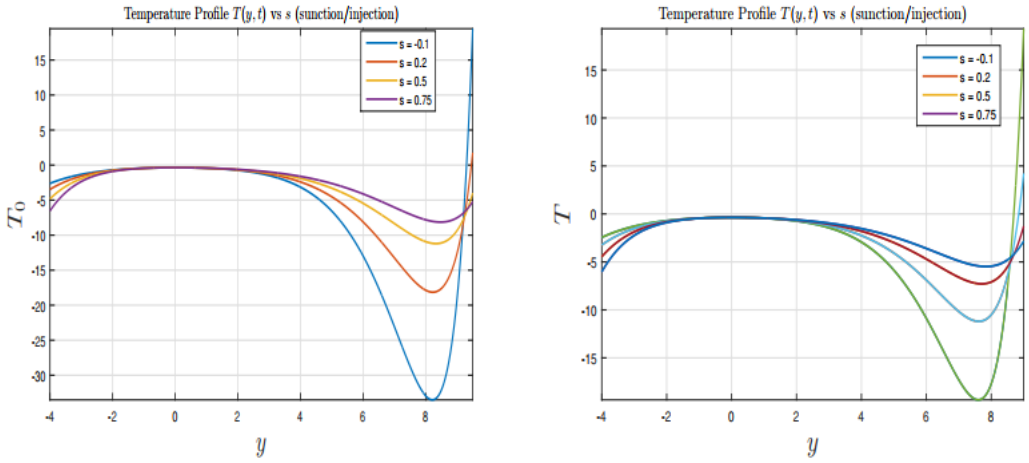


FIGURE 3. Temperature profiles for different values of s at $t = 0$ and $t = 0.25$ respectively for fixed values of G_r, P_r.

Now, we observe the effect of Prandtl number P_r.

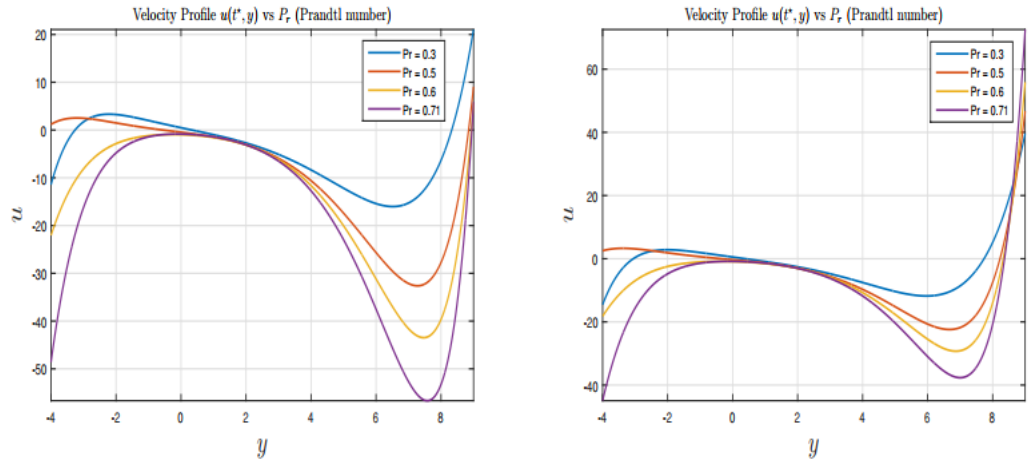


FIGURE 4. Velocity profiles for different values of P_r at $t = 0$ and $t = 0.25$ respectively for fixed values of s, G_r.

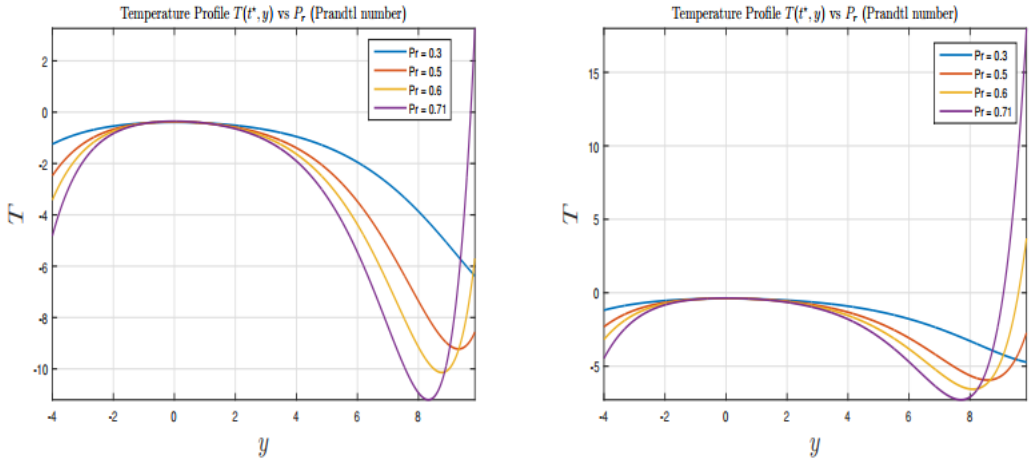


FIGURE 5. Temperature profiles for different values of P_r at $t = 0$ and $t = 0.25$ respectively for fixed values of s, G_r.

Now, the effect of Grashof number Gr on the velocity and temperature profiles. It is observed for negative values of s, indicating injection, there is rapid change in the temperature profile which led to significant variation. This indicate that when incompressible fluid is injected into the system, this could lead to the significant rise in the temperature of the system.

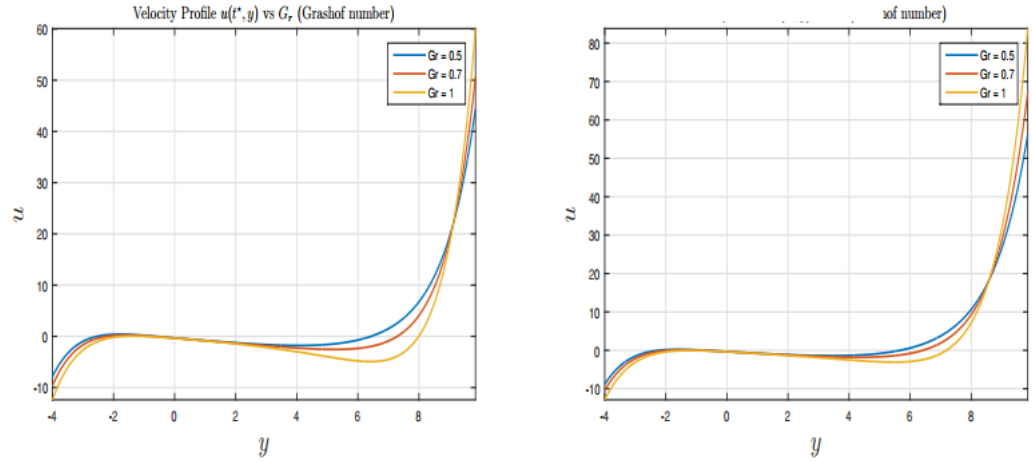


FIGURE 6. Velocity profiles for different values of G_r at $t = 0$ and $t = 0.25$ respectively for fixed values of s, P_r.

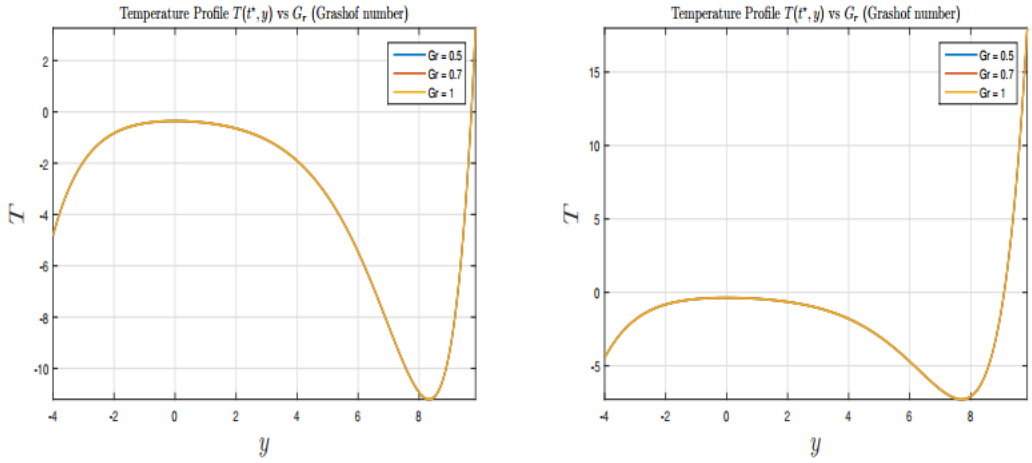


FIGURE 7. Temperature profiles for different values of G_r at $t = 0$ and $t = 0.25$ respectively for fixed values of s, P_r.

Accelerated case. Firstly, we study the effect of suction parameter, just as shown in the figure 8. One observes significant variation in both temperature and velocity profiles. Next, with the same fixed parameters, we vary the Grashof number *Gr*.

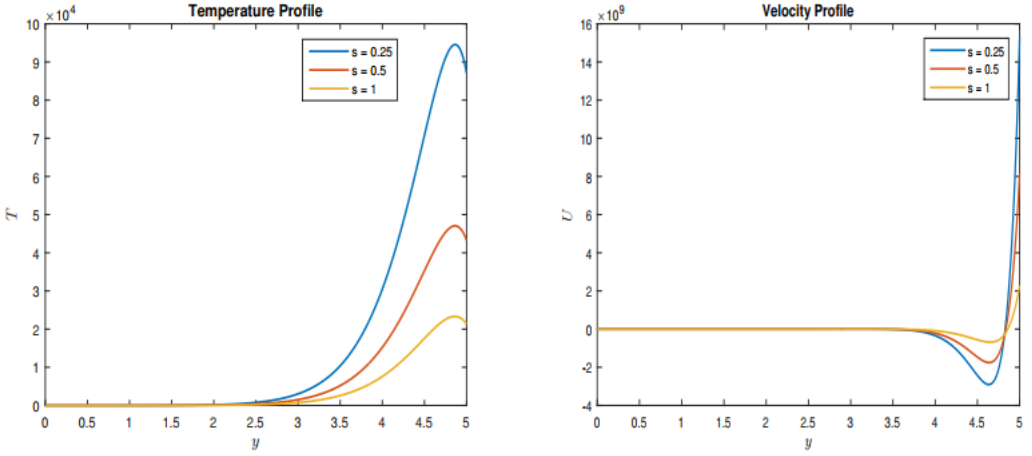


FIGURE 8. Temperature and Velocity profiles for s at $t = 1$ and for fixed values of $Gr = 0.5, P_r = 0.2, \alpha_1 = 0.2, \alpha_2 = 0.5, \alpha = 1, \gamma_0 = 1, \mu_0 = 0.5 = \mu, p_0 = 1, s_0 = 1$ with varying suction parameter $s = 0.25, 0.5, 1$.

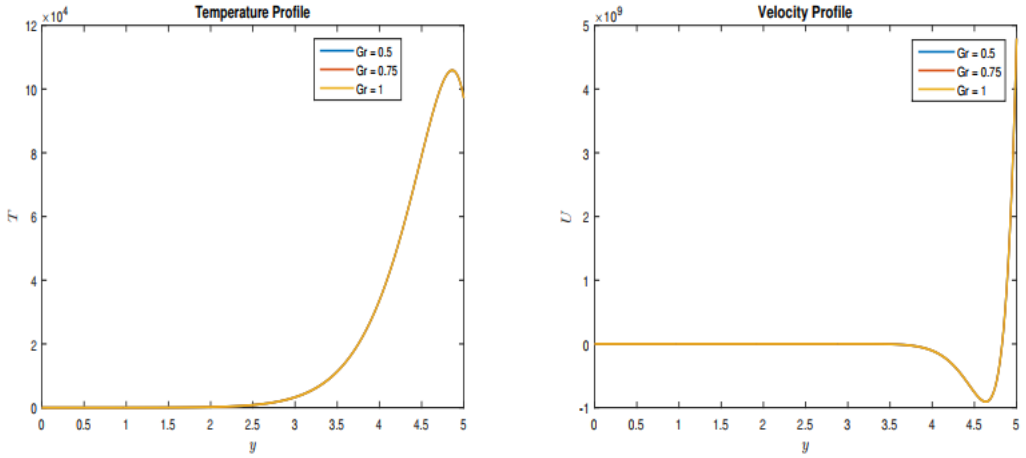


FIGURE 9. Temperature and Velocity profiles for G_r at $t = 1$ and for fixed values of $s = 0.25, P_r = 0.2, \alpha_1 = 0.75, \alpha_2 = 1, \alpha = 1, \gamma_0 = 1, \mu_0 = 0.5 = \mu, p_0 = 1, s_0 = 1$ with varying Grashof number $s = 0.5, 0.75, 1$.

Using the same fixed parameters, we vary the Prandtl number P_r. The figures in 10 show we lost track of the effects of the Prandtl numbers 0.2 and 0.5. This could be due to the numerical errors that if analytical method is employed can be avoided. Similar observation and conclusions can be made on Figure 9.

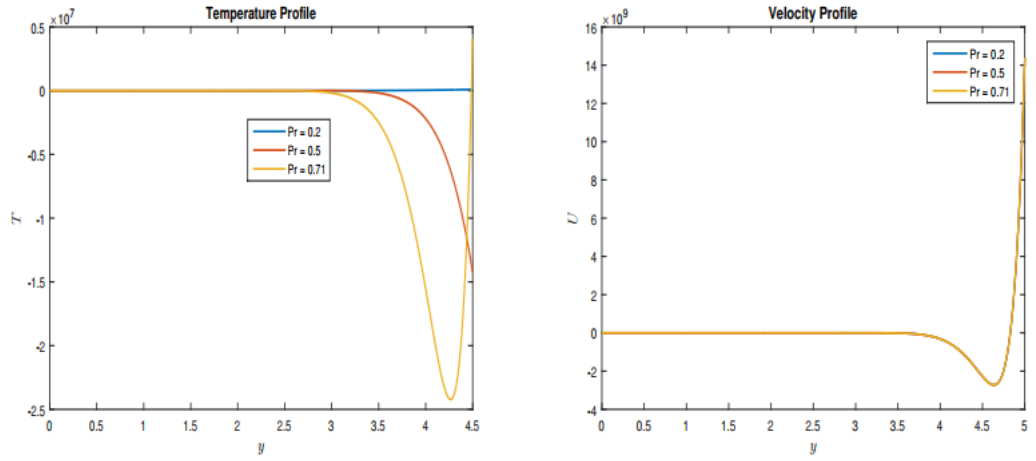


FIGURE 10. Temperature and Velocity profiles for P_r at $t = 1$ and for fixed values of $Gr = 0.5, s = 0.25, \alpha_1 = 0.2, \alpha_2 = 0.5, \alpha = 1, \gamma_0 = 1, \mu_0 = 0.5 = \mu, p_0 = 1, s_0 = 1$ with varying Prandtl number $P_r = 0.2, 0.5, 0.71$.

Discussion

The results reveal that increase in the Grashof number G_r enhances buoyancy forces, leading to a significant increase in velocity profiles, consistent with finding as found

in Alkanhal et. al. (2018). However, compared to previous studies, particularly of Jah et al. (2018), the present work shows more pronounced transient response under impulsive motion, highlighting the importance of time-dependent modelling.

The Prandtl number P_r is observed to inversely affect thermal boundary layer thickness. This aligns with the classical heat transfer theory but also demonstrates sharper gradients under accelerated motion conditions, which are often overlooked in steady-state analyses. This is evident from the Figures Fig. 6 and Fig. 7.

The inclusion of suction/injection reveals stabilizing and destabilizing effects depending on parameter magnitude. Unlike earlier works of Gorla and Sidawi (2020), this study shows that suction significantly reduces thermal boundary thickness in transient regimes. This is based on the results shown in Figure **2** and **3**.

Finally, the key advancement obtained lies in the application of Talbot's Method, which provides an improved stability compared to the traditional inversion methods, faster convergence in evaluating temperature and velocity fields, reduced computational error. Our contributions extends MHD free convection theory to fully transient regimes and validates the Talbot inversion as a reliable computational tool in fluid mechanics. This shows practical applicability to cooling systems, boundary-layer control, and energy sytems. The MATLAB implementation ensures the reproducibility for parameter validation against results.

Conclusion

This study provides a detailed analysis of incompressible fluid flow and heat transfer using Laplace transform and analytical techniques. The effects of suction/injection parameter, Prandtl number, and Grashof number on velocity and temperature profiles were systematically examined. The Talbot's method appeared to provide a reliable way to compute inverse Laplace transforms numerically as analytical approach is not easily available. The method implementation ensures numerical stability by modifying the contour integration and parameter selection. MATLAB codes is generated and tested with various values of P_r, G_r, and s to guarantee robustness. The results demonstrate that Laplace transform methods are effective in solving similar fluid flow systems and offer insights into parameter-dependent behaviours.

Future work could extend this analysis to higher, say 3, dimensional flows or incorporate more complex boundary conditions to simulate real-world scenarios.

References

Abate, J., & Valkó, P. P. (2004). Multi-precision Laplace transform inversion. *International Journal for Numerical Methods in Engineering, 60*(5), 979–993. https://doi.org/10.1002/nme.995

Abbas, Z., Abdal, S., Hussain, N., Hussain, F., Adnan, M., Ali, B., Zulqarnain, R. M., Ali, L., & Younas, S. (2019). MHD boundary layer flow and heat transfer of nanofluid over a vertical stretching sheet in the presence of a heat source. *Scientific Inquiry and Review, 3*(4), 60–73. https://doi.org/10.32350/sir.34.05

Ahmed, Z., Nadeem, S., Saleem, S., & Ellahi, R. (2019). Numerical study of unsteady flow and heat transfer CNT-based MHD nanofluid with variable viscosity over a permeable shrinking surface. *International Journal of Numerical Methods for Heat & Fluid Flow, 29*(12), 4607–4623. https://doi.org/10.1108/HFF-04-2019-0346

Alkanhal, T. A., Sheikholeslami, M., Arabkoohsar, A., Haq, R., Shafee, A., Li, Z., & Tlili, I. (2019). Simulation of convection heat transfer of magnetic nanoparticles including entropy generation using CVFEM. *International Journal of Heat and Mass Transfer, 136*, 146–156. https://doi.org/10.1016/j.ijheatmasstransfer.2019.02.095

Amanifard, M., Borji, M., & Haghi, A. K. (2007). Heat transfer in porous media. *Brazilian Journal of Chemical Engineering, 24*(2), 223–232. https://doi.org/10.1590/S0104-66322007000200007

Aziz, S., Ahmad, I., Khan, S. U., & Ali, N. (2021). A three-dimensional bioconvection Williamson nanofluid flow over bidirectional accelerated surface with activation energy and heat generation. *International Journal of Modern Physics B, 35*(9), Article 2150132. https://doi.org/10.1142/S0217979221501320

Bejan, A. (2013). *Convection heat transfer* (4th ed.). Wiley. https://doi.org/10.1002/9781118671627

Chamkha, A. J. (1997). MHD-free convection from a vertical plate embedded in a thermally stratified porous medium with Hall effects. *Applied Mathematical Modelling, 21*(10), 603–609. https://doi.org/10.1016/S0307-904X(97)00084-X

Dharmaiah, G., Vedavathi, N., Rani, C. B., & Balamurugan, K. (2018). MHD boundary layer flow and heat transfer of a nanofluid past a radiative and impulsive vertical plate. *Frontiers in Heat and Mass Transfer, 11*(1), 1–7. https://doi.org/10.5098/hmt.11.14

Dogonchi, A. S., & Hashim. (2019). Heat transfer by natural convection of Fe3O4-water nanofluid in an annulus between a wavy circular cylinder and a rhombus. *International Journal of Heat and Mass Transfer, 130*, 320–332. https://doi.org/10.1016/j.ijheatmasstransfer.2018.10.086

Gaurav, & Shankar, V. (2007). Stability of gravity-driven free-surface flow past a deformable solid at zero and finite Reynolds number. *Physics of Fluids, 19*(2), Article 024105. https://doi.org/10.1063/1.2698582

Gebhart, B. (1962). *Heat transfer*. McGraw-Hill.

Gorla, R. S. R., & Sidawi, I. (1994). Free convection on a vertical stretching surface with suction and blowing. *Applied Scientific Research, 52*, 247–257. https://doi.org/10.1007/BF00853952

Hayat, T., Bibi, A., Yasmin, H., & Alsaadi, F. E. (2018). Magnetic field and thermal radiation effects in peristaltic flow with heat and mass convection. *Journal of Thermal Science and Engineering Applications, 10*(5), Article 051018. https://doi.org/10.1115/1.4040282

Ibrahim, W., & Makinde, O. D. (2015). Magnetohydrodynamic stagnation point flow and heat transfer of Casson nanofluid past a stretching sheet with slip and convective boundary condition. *Journal of Aerospace Engineering, 29*(2), Article 04015037. https://doi.org/10.1061/(ASCE)AS.1943-5525.0000529

Jha, B. K., Azeez, L. A., & Oni, M. O. (2019). Unsteady hydromagnetic-free convection flow with suction/injection. *Journal of Taibah University for Science, 13*(1), 136–145. https://doi.org/10.1080/16583655.2018.1545624

Kays, W. M., & Crawford, M. E. (1993). *Convective heat and mass transfer* (3rd ed.). McGraw-Hill.

Khan, M. I., Hafeez, M. U., Hayat, T., Khan, M. I., & Alsaedi, A. (2020). Magneto rotating flow of hybrid nanofluid with entropy generation. *Computer Methods and Programs in Biomedicine, 183*, Article 105093. https://doi.org/10.1016/j.cmpb.2019.105093

Krishna, M. V., & Chamkha, A. J. (2019). MHD peristaltic rotating flow of a couple stress fluid through a porous medium with wall and slip effects. *Special Topics & Reviews in Porous Media: An International Journal, 10*(3), 245–258. https://doi.org/10.1615/SpecialTopicsRevPorousMedia.2019028609

Makinde, O. D. (2018). Unsteady MHD flow of radiating and rotating fluid with Hall current and thermal diffusion past a moving plate in a porous medium. *Defect and Diffusion Forum, 389*, 71–85. https://doi.org/10.4028/www.scientific.net/DDF.389.71

Moon, J. H., Lee, J., & Lee, S. H. (2022). Numerical study of the boiling heat transfer characteristics of bluff body quenching in cylindrical tube. *Case Studies in Thermal Engineering, 32*, Article 101900. https://doi.org/10.1016/j.csite.2022.101900

Muhammad, A. L., Baffa, A. B., & Dauda, U. M. (2016). Transient airflow process across three vertical vents induced by stack-driven effect inside un-stratified cross-ventilated rectangular building with an opposing flow in one of the upper opening. *International Journal of Computer Applications, 148*(1), 4–11. https://doi.org/10.5120/ijca2016910676

Nadeem, M., Siddique, I., Bilal, M., & Anjum, K. (2024). Numerical study of MHD Prandtl Eyring fuzzy hybrid nanofluid flow over a wedge. *Numerical Heat Transfer, Part A: Applications, 85*(24), 4328–4344. https://doi.org/10.1080/10407782.2023.2257379

Ostrach, S. (1988). Natural convection in enclosures. *Journal of Heat Transfer, 110*(4b), 1175–1190. https://doi.org/10.1115/1.3250619

Özisik, M. N. (1993). *Heat conduction* (2nd ed.). Wiley.

Padmavathi, L. (2023). Oscillatory plate temperature and unsteady free convection flow of an suction/injection parameter on MHD in a vertical channel. *International Journal of*

Research Publication and Reviews, 4(10), 2478–2485. https://ijrpr.com/uploads/V4ISSUE10/IJRPR18421.pdf

Schlichting, H. (1979). *Boundary-layer theory* (7th ed.). McGraw-Hill.

Sene, N. (2022). Second-grade fluid with Newtonian heating under Caputo fractional derivative: Analytical investigations via Laplace transforms. *Mathematical Modelling and Numerical Simulation with Applications, 2*(1), 13–25. https://doi.org/10.53391/mmnsa.2022.01.002

Tlili, I., Ramzan, M., Kadry, S., Kim, H.-W., & Nam, Y. (2020). Radiative MHD nanofluid flow over a moving thin needle with entropy generation in a porous medium with dust particles and Hall current. *Entropy, 22*(3), Article 354. https://doi.org/10.3390/e22030354

Waqas, H., Farooq, U., Naseem, R., Hussain, S., & Alghamdi, M. (2021). Impact of MHD radiative flow of hybrid nanofluid over a rotating disk. *Case Studies in Thermal Engineering, 26*, Article 101015. https://doi.org/10.1016/j.csite.2021.101015

Weideman, J. A. C. (2006). Optimizing Talbot's contours for the inversion of the Laplace transform. *SIAM Journal on Numerical Analysis, 44*(6), 2342–2362. https://doi.org/10.1137/050625837

White, F. M. (2006). *Viscous fluid flow* (3rd ed.). McGraw-Hill.